European Journal of Radiology Open 8 (2021) 100312

Contents lists available at ScienceDirect

European Journal of Radiology Open

journal homepage: www.elsevier.com/locate/ejro

Quantitative evaluation of focal liver lesions with T1 mapping using a phase-sensitive inversion recovery sequence on gadoxetic acid-enhanced MRI

Motohira Mio [a,*], Yasuhiro Fujiwara [b], Kazuki Tani [a], Tatsuo Toyofuku [a], Toshihiro Maeda [a], Toshiro Inoue [a]

[a] Department of Radiology, Fukuoka University Chikushi Hospital, 1-1-1 Zokumyoin, Chikushino, 818-8502, Japan
[b] Department of Medical Image Sciences, Faculty of Life Sciences, Kumamoto University, 4-24-1, Kuhonji, Chuo-ku, Kumamoto, 862-0976, Japan

ARTICLE INFO

Keywords:
Magnetic resonance imaging (MRI)
Gadoxetic acid-enhanced MRI
Liver
Phase-sensitive inversion recovery (PSIR)
T1 mapping

ABSTRACT

Purpose: To determine the usefulness of T1 values measured using a phase-sensitive inversion recovery (PSIR) sequence for the diagnosis of focal liver lesions.
Method: The study enrolled 87 patients who underwent gadoxetic acid-enhanced magnetic resonance imaging (MRI) for assessment of 38 hepatocellular carcinomas, 33 hepatic hemangiomas, 30 metastatic liver tumors, and 14 hepatic cysts. PSIR was performed before and 15 min after contrast agent administration, and then the respective T1 values were measured and the T1 reduction rate was calculated. Wilcoxon matched-pairs signed-rank test was used to compare T1 values pre- and post-contrast administration in each tumor. The Kruskal-Wallis test and Dunn's post-hoc test were used to compare T1 values among all tumors pre- and post-contrast administration and the T1 reduction rate among all tumors.
Results: The T1 values measured before and after contrast enhancement were 1056 ± 292 ms and 724 ± 199 ms for hepatocellular carcinoma, 1757 ± 723 ms and 1033 ± 406 ms for metastatic liver tumor, 2524 ± 908 ms and 1071 ± 390 ms for hepatic hemangioma, and 3793 ± 207 ms and 3671 ± 241 ms for liver cysts, respectively. The T1 values obtained before and after contrast administration showed significant differences for all tumors except liver cysts ($P < 0.0001$). T1 reduction rate was not significantly different between hepatocellular carcinoma and metastatic liver tumor, but was significantly different among other tumors ($P < 0.05$).
Conclusions: T1 mapping using the PSIR sequence is useful to differentiate focal liver lesions.

1. Introduction

Gadoxetic acid is widely used as a liver-specific contrast agent for differentiating focal liver tumors [1–7]. Gadoxetic acid not only enables vascularity assessment during dynamic studies but also increases the T1 contrast between normal liver parenchyma and tumor in the hepatobiliary phase (HBP). However, uptake of gadoxetic acid into liver parenchyma is reduced by impaired liver function, which may cause focal liver lesions to be missed [8,9]. Although most malignant liver lesions present with hypointensity in the HBP, benign liver lesions such as hemangiomas also show hypointensity in the HBP, making it difficult to distinguish these lesions [10–12]. For this reason, various methods for differentiating focal liver lesions have been investigated and reported [13–16].

T1 mapping enables quantification of T1 values for comparisons across images, and the usefulness of focal liver lesion differentiation using T1 values has been reported [17–19]. However, the conventional T1 mapping method still has problems related to versatility and T1 measurement accuracy [20,21]. In contrast, T1 mapping using phase-sensitive inversion recovery (PSIR) has been validated in studies of phantoms and healthy subjects, and has been reported to have high T1 value measurement accuracy [22]. Furthermore, the use of PSIR for T1 mapping has been frequently employed for cardiac magnetic resonance imaging (MRI) recently, and this approach may be applied to various

Abbreviations: AUC, area under the ROC curve; CT, computed tomography; HBP, hepatobiliary phase; HCC, hepatocellular carcinoma; MRI, magnetic resonance imaging; PSIR, phase-sensitive inversion recovery; ROC, receiver operating characteristic; ROI, region of interest; SI, signal intensity.

* Corresponding author.
E-mail address: mio@fukuoka-u.ac.jp (M. Mio).

https://doi.org/10.1016/j.ejro.2020.100312
Received 9 October 2020; Received in revised form 4 December 2020; Accepted 7 December 2020

regions due to its high versatility [23,24].

In this study, we measured the T1 values of focal liver lesions using PSIR before and after gadoxetic acid injection, examining the usefulness of T1 mapping using PSIR in the differential diagnosis of focal liver lesions.

2. Materials and methods

2.1. Subjects

This study was approved by our Institutional Review Board, and written informed consent was obtained from all participants before the MR examinations. We enrolled 183 patients who underwent gadoxetic acid-enhanced MRI at our hospital from May 2018 to October 2019. We excluded patients with liver lesions that had not been confirmed by computed tomography (CT) and/or MRI. After applying this criteria, a total of 87 patients (50 men, 37 women; age range, 35–91 years; mean age, 69 ± 13 years) were enrolled in this study, including 28 patients (16 men, 12 women) diagnosed with 38 hepatocellular carcinomas (HCCs), 27 patients (19 men, 8 women) diagnosed with 33 hepatic hemangiomas, 21 patients (10 men, 11 women) diagnosed with 30 metastatic liver tumors, and 11 patients (4 men, 7 women) diagnosed with 14 liver cysts (Fig. 1). No magnetic resonance (MR) examinations were performed for other tumors in this study. The primary metastatic liver tumors were colorectal cancers in all patients. All of the liver lesions were diagnosed on the basis of typical CT and/or MRI features.

2.2. MRI protocol

All studies were performed on a 3.0-T clinical MRI system (Ingenia, Philips Healthcare, Best, the Netherlands) with a 32-channel phased-array body receiver coil. First, all patients underwent two-dimensional T1-weighted fast gradient-echo (GRE) in phase and opposed phase, T2-weighted turbo spin-echo, diffusion-weighted imaging, and T1-weighted three-dimensional (3D) fast GRE sequences based on the standard liver MR examination protocol at our institution. Details of the MR parameters of the respective sequences are shown in Table 1. Second, for T1 mapping, PSIR was performed before and 15 min after injection of gadoxetic acid consistently in each patient. The T1 mapping method using the PSIR sequence has been described in a previous report [22]. The major characteristic of the PSIR is the 3D turbo field echo (TFE) readouts at the two inversion times (TIs) after applying a non-selective adiabatic inversion recovery pulse. The T1 values were estimated using two TI images acquired from the inversion recovery-prepared data and reference data with the same flip angle (FA). The imaging parameters were as follows: repetition time, 20 ms; echo time (TE), 1.82, 5.82, 9.82, 13.82, and 17.82 ms; TFE factor, 35; FA, 10°; shot interval, 1500 ms; TIs, 500 and 2500 ms; field of view, 360 × 300 mm^2; matrix, 180 × 120; slice thickness, 6 mm; number of slabs, 1; number of slices, 5; acceleration factor, 2; k-space profile ordering, low–high; fat-suppression, spectral pre-saturation with inversion recovery; and scan time, 13.5 s (a single breath-hold). Although PSIR can be used to measure not only the T1 value but also the T2* value acquired with multi TEs, we did not measure T2* values in this study. All patients were administered body weight-adjusted (0.025 mmol/kg) doses of gadoxetic acid as bolus injections in 4 s.

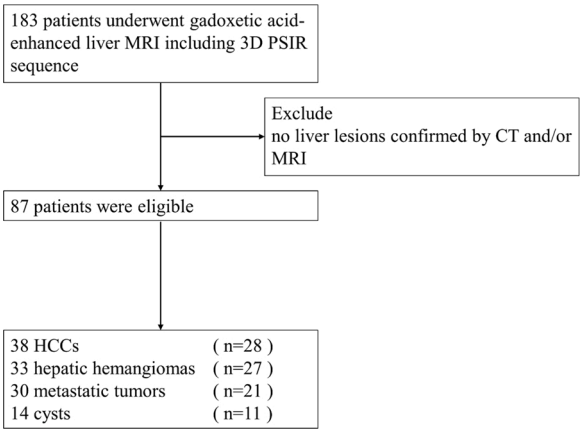

Fig. 1. Flowchart of the study population.

2.3. Image analysis

We measured the T1 values of the focal liver lesions of each patient. The region of interest (ROI) was set on the lesions as precisely as possible, and the T1 value was obtained on a T1 map (Fig. 2). The T1 reduction ratios were calculated using pre-contrast and post-contrast T1 values as follows:

T1 reduction ratio = (pre-T1 value – post-T1 value) / pre-T1 value × 100

The ROIs were defined by one of the authors (M. M. with more than 10 years of experience with MRI). T1 maps were generated using image-processing software (MATLAB2015a, MathWorks, Natick, MA, USA). The specific calculation method of the T1 value was the same as that reported previously, and the T1 value was calculated based on the relationship between the two IR magnetization evolutions [22].

2.4. Statistical analyses

Statistical analyses were performed using Prism 6.0 (GraphPad software, La Jolla, CA, USA). We compared pre-contrast and post-contrast T1 values in each focal liver lesion using the Wilcoxon matched-pairs signed-rank test. The Kruskal-Wallis test with Dunn's post-hoc test for multiple comparisons was used to analyze the differences in pre-contrast T1 values, post-contrast T1 values, and T1 reduction rates among focal liver lesions. Additionally, receiver operating characteristic (ROC) curves were used to determine T1 cut-off values for optimal differentiation among focal liver lesions. The diagnostic performance for differentiating focal liver lesions were evaluated by calculating the area under the ROC curve (AUC), and the optimal T1 cut-off values were calculated with Youden index. A P value less than 0.05 was considered to indicate a significant difference for each tests.

3. Results

The pre- and post-contrast T1 values and T1 reduction rates are shown in Table 2. Liver cysts showed the longest pre- and post-contrast T1 values, and the shortest pre- and post-contrast T1 values were observed for HCC. The T1 reduction rate was the highest for hepatic hemangiomas and lowest for liver cysts. HCCs, hepatic hemangiomas, and metastatic liver tumors showed shortened T1 values after injection of gadoxetic acid, with significant differences between pre- and post-contrast T1 values (Fig. 3). The Kruskal-Wallis test with Dunn's multiple comparisons test showed no significant difference in the pre-contrast T1 value between hepatic hemangioma and liver cyst ($P = 0.076$) or the post-contrast T1 value between hepatic hemangioma and metastatic liver tumor ($P > 0.99$). The T1 reduction rate was not significantly different between HCC and metastatic liver tumors ($P = 0.66$). The comparisons of other combinations of focal liver lesions showed statistically significant differences (Fig. 4). Table 3 shows the T1 cut-off values between each pair of focal liver lesions determined by the ROC analysis.

4. Discussion

In this study, we applied T1 mapping using PSIR to measure T1 values of focal liver lesions. Although MR signal intensity (SI) does not

Table 1
Imaging parameters of liver MR examination protocol.

Sequence	T1 2D FFE	DWI	T2W-TSE	T1 3D TFE
Imaging plane	Transverse	Transverse	Transverse	Transverse
Field of view (mm^2)	350 × 300	350 × 300	350 × 300	350 × 300
Matrix	220 × 222	124 × 161	312 × 256	248 × 212
Number of slices	20	20	20	100
Slice thickness (mm)	8	8	8	2
Repetition time (ms)	149	5500	2160	2.9
Echo time (ms)	1.15 (opposed phase) 2.3 (in phase)	83	75	1.41
Flip angle (degree)	60	90	90	11
Echo train length/ Turbo factor	N/A	N/A	32	47
Number of signal averages	1	1	1	1
Fat suppression	N/A	Spectral fat suppression (SPAIR)	Spectral fat suppression (SPIR)	Spectral fat suppression (SPAIR) (SPAIR)
Total scan duration	15.2 s	2 m 56 s	1 m 48 s	14.7 s

T1 2D FFE, T1-weighted two dimensional fast field echo; DWI, diffusion-weighted imaging; T2W-TSE, T2-weighted turbo spin-echo; T1 3D TFE, T1-weighted three dimensional turbo field echo; N/A, not applicable; SPAIR, spectral attenuated inversion recovery; SPIR, spectral pre-saturation with inversion recovery.

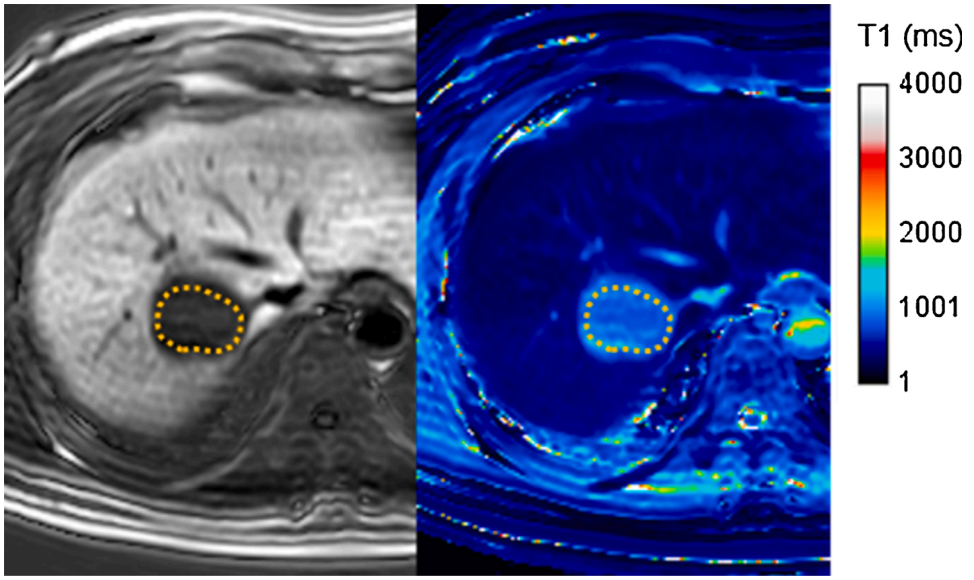

Fig. 2. Setting of region of interest (ROI) in the focal liver lesion on the T1 mapping image to measure the T1 value. The ROI was set as precisely as possible on the focal liver lesion.

Table 2
T1 values measured by PSIR and the calculated T1 reduction rates.

	T1 value (ms)		T1 reduction rate (%)	*P* value *
	Pre-contrast	Post-contrast		
HCC	1056 ± 292	724 ± 199	30 ± 12	< 0.0001
Hemangioma	2524 ± 908	1071 ± 390	57 ± 11	< 0.0001
Metastatic tumor	1757 ± 723	1033 ± 406	38 ± 16	< 0.0001
Cyst	3793 ± 207	3671 ± 241	3 ± 4	0.38

* Comparison with pre- and post-contrast T1 values.

correlate linearly with the concentration of contrast agent, a change in the longitudinal relaxation rate (1/T1) is directly proportional to the concentration of the contrast agent in the tissue [25]. As such, it is important to measure T1 values of focal liver lesions. Additionally, T1 mapping may serve as a quantitative assessment method that is less affected by MR parameters and MR systems than SI measurements [26–28]. However, there are some problems in the conventional T1 mapping method. The dual FA method requires two optimal FAs, and it is necessary to know the T1 value to be measured in advance [20]. The Lock-Locker method shows high T1 value dependence, because of which the measurement error increases as the T1 value becomes longer [21]. By contrast, PSIR applied in this study is less dependent on the T1 value, offering the advantage of more accurate T1 measurements than the conventional T1 mapping method [22].

Furthermore, because PSIR uses a non-selective adiabatic inversion recovery pulse, measured T1 values may be less susceptible to B1 inhomogeneity than those of the dual FA method. In addition, another advantage of PSIR is its feasibility in clinical practice because it is a sequence commonly used in the cardiac area [23,24]. These findings suggest that T1 mapping using PSIR can be applied in various body regions due to its high measurement accuracy and versatility.

According to Table 1, the pre-contrast T1 values for HCC and metastatic liver tumors were 1056 ± 292 ms and 1757 ± 723 ms, respectively. These values were close to those of a previous study, suggesting that T1 mapping using PSIR yields reproducible results that are similar to those of previously reported methods [19]. On the contrary, the T1 values for liver cysts and hepatic hemangiomas were longer than those for HCCs and metastatic liver tumors. The results could be explained by the abundance of liquid components inside these tumors [29]. A previous study reported that the pre-contrast T1 value for hepatic hemangioma was 1432 ± 600 ms [19]. The pre-contrast T1 value of hepatic hemangiomas measured using PSIR was 2524 ± 908 ms, which was longer than the previously reported value. The conventional T1 mapping

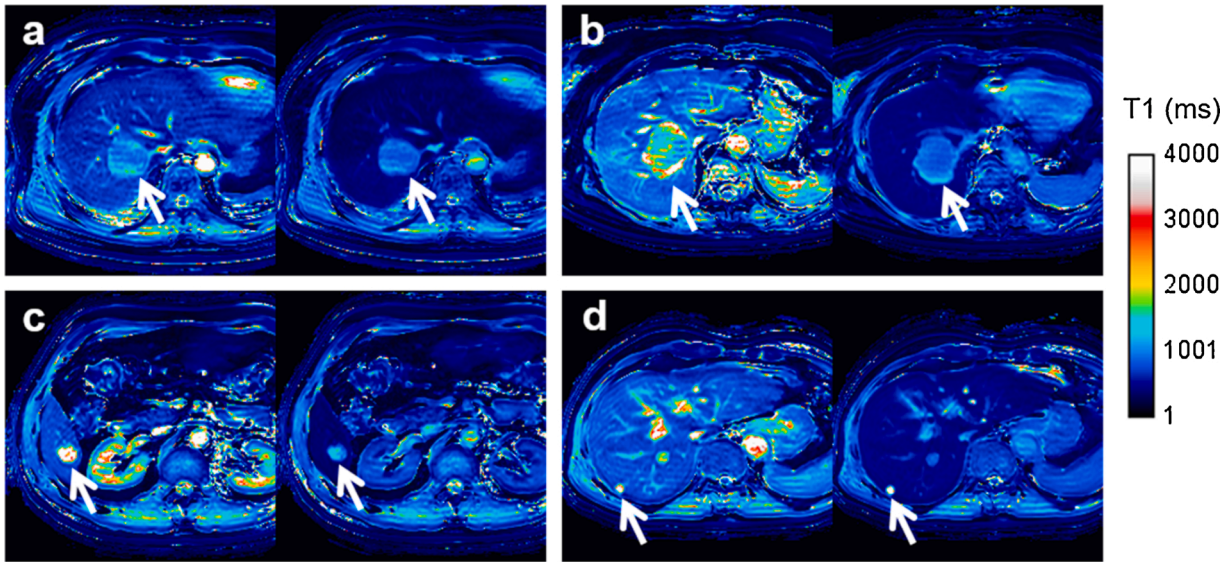

Fig. 3. Representative T1 mapping images obtained using phase-sensitive inversion recovery before (left side) and after contrast agent administration (right side) in patients with (a) hepatocellular carcinomas, (b) metastatic tumor, (c) hemangioma, and (d) cyst.

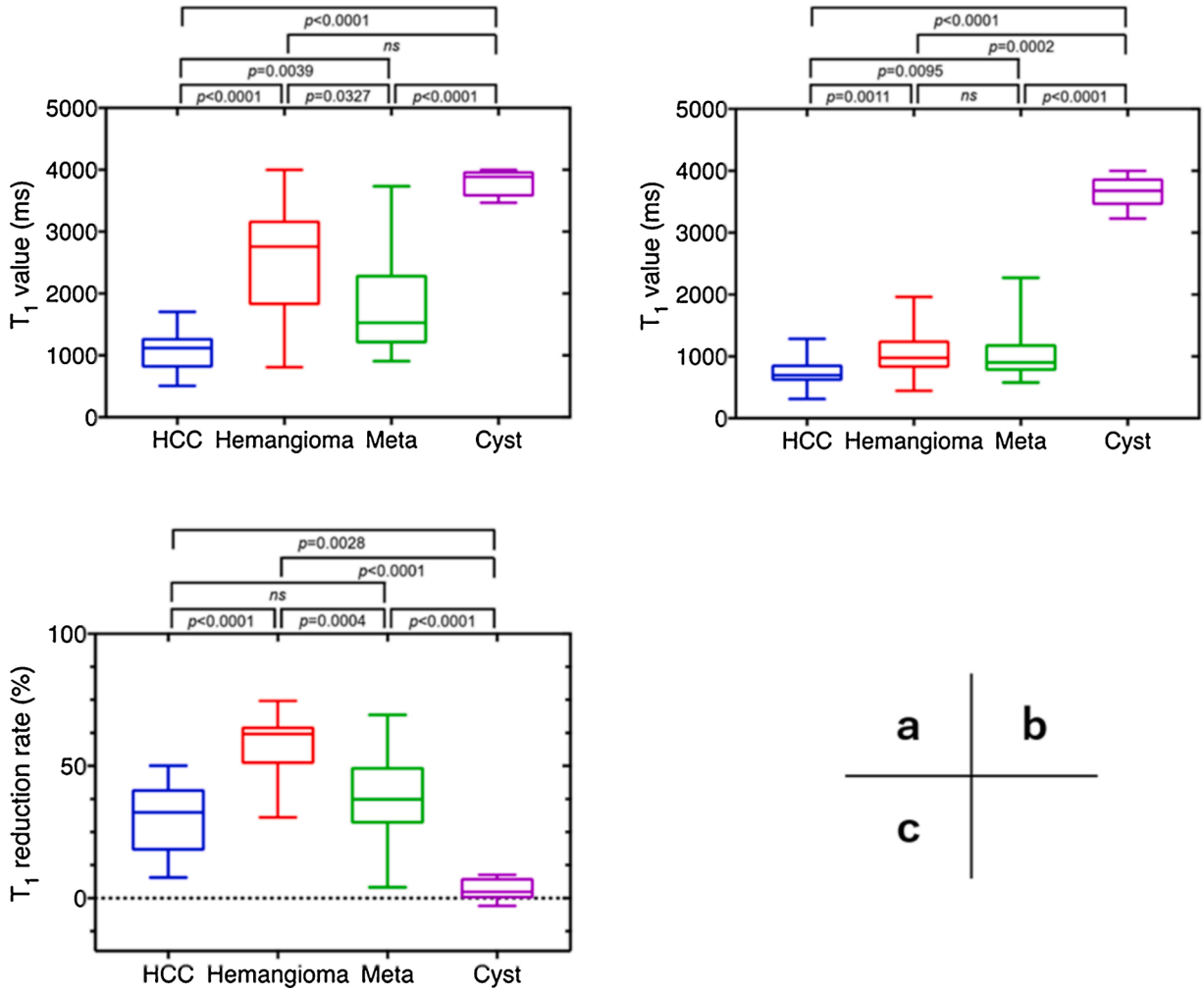

Fig. 4. Results of multiple comparisons among focal liver lesions. (a) Pre-contrast T1 value, (b) post-contrast T1 value, and (c) T1 reduction rate.

Table 3
Diagnostic ability of T1 mapping using PSIR by ROC analysis.

	Pre-contrast T1 value (ms)				Post-contrast T1 value (ms)				T1 reduction rate (%)			
	AUC	Specificity	Sensitivity	Cut-off	AUC	Specificity	Sensitivity	Cut-off	AUC	Specificity	Sensitivity	Cut-off
HCC vs. hemangioma	0.947	1.000	0.848	> 1742	0.788	0.605	0.879	> 716	0.947	1.000	0.788	> 50
95% CI	0.891–1.000	0.908–1.000	0.691–0.934		0.678–0.898	0.447–0.744	0.727–0.952		0.900–0.995	0.908–1.000	0.623–0.893	
HCC vs. metastatic tumor	0.817	0.868	0.633	> 1325	0.757	0.658	0.767	> 769	0.639	0.421	0.867	> 26
95% CI	0.717–0.917	0.727–0.943	0.455–0.781		0.642–0.872	0.499–0.788	0.591–0.882		0.505–0.774	0.279–0.578	0.703–0.947	
HCC vs. cyst	1.000	1.000	1.000	> 2586	1.000	1.000	1.000	> 2246	0.977	0.974	0.929	< 10
95% CI	1.000–1.000	1.000–1.000	1.000–1.000		1.000–1.000	1.000–1.000	1.000–1.000		0.938–1.000	0.865–0.999	0.685–0.996	
Hemangioma vs. metastatic tumor	0.772	0.849	0.600	< 1742	0.544	0.576	0.567	< 940	0.836	0.970	0.600	< 39
95% CI	0.655–0.889	0.691–0.934	0.423–0.754		0.401–0.688	0.408–0.728	0.392–0.726		0.734–0.939	0.847–0.998	0.423–0.754	
Hemangioma vs. cyst	0.903	0.849	1.000	> 3387	1.000	1.000	1.000	> 2585	1.000	1.000	1.000	< 25
95% CI	0.811–0.994	0.691–0.934	0.785–1.000		1.000–1.000	0.896–1.000	0.785–1.000		1.000–1.000	0.896–1.000	0.785–1.000	
Metastatic tumor vs. cyst	0.988	0.967	1.000	> 3159	1.000	1.000	1.000	> 2740	0.971	0.900	1.000	< 20
95% CI	0.962–1.000	0.833–0.998	0.785–1.000		1.000–1.000	0.896–1.000	0.785–1.000		0.930–1.000	0.744–0.965	0.785–1.000	

CI: confidence interval.

method has a high T1 value dependence, with the measurement accuracy decreasing as the T1 value increases. By contrast, PSIR shows low dependence on the T1 value, allowing accurate measurements of long T1 values compared to the conventional T1 mapping method [22]. Therefore, it was suggested that PSIR could estimate T1 values of hepatic hemangiomas accurately, whereas conventional methods could be underestimating them.

The T1 reduction rates of HCCs and hepatic hemangiomas calculated in this study were not different from those reported in a previous study, but the rate for metastatic liver tumors was higher than that in a previous study [18]. This could be explained by the fact that all primary metastatic liver tumors targeted in this study were colorectal cancers, and 72 % of colorectal cancer liver metastases show mixed SI in HBP, in terms of the expected gadoxetic acid uptake [30]. For this reason, it is conceivable that the T1 reduction rate calculated in this study was higher.

In this study, we investigated multiple comparisons among the four focal liver lesions. The results showed that pre-contrast T1 values of hepatic hemangiomas and liver cysts and the T1 reduction rates of HCC and metastatic liver tumors showed no significant differences. In other words, the differential diagnosis of focal liver lesions is difficult with pre-contrast T1 value or T1 reduction rate alone, although combinations of these values can facilitate differentiation of focal liver lesions. Hepatic hemangioma is distinguished by high pre-contrast T1 value and T1 reduction rate. When distinguishing metastatic liver tumors from HCC, the following conditions are more likely to indicate metastatic liver tumor: 1) T1 reduction rate lower than 40 %, 2) pre-contrast T1 value higher than 1325 ms (Table 2). Collectively, our data obtained using PSIR indicate that it plays an important role in the differential diagnosis of focal liver lesions.

This study has some limitations. First, this study examined only four types of focal liver lesions. It is a general belief that the differential diagnosis for hypervascular liver lesions (such as focal nodular hyperplasia, hepatic adenoma) is important in clinical practice, although previous studies have not revealed whether these lesions can be differentiated by T1 mapping. Further studies on T1 mapping using PSIR with more patients and a greater variety of liver lesions are required to address this question. Second, the number of focal liver lesions was small, and diagnosis of these lesions was performed using typical imaging findings. In other words, the diagnosis may be incorrect for cases with less typical imaging findings, which may have affected the results of this study. Third, the acquisition times with breath-hold were long. Elderly people cannot hold their breath until the end time, causing motion artifacts. This may have affected the T1 values of T1 mapping. However, we think that the problem of acquisition times can be solved by applying higher acceleration imaging technology and compression sensing, which have been reported in recent years [31,32].

5. Conclusion

The PSIR sequence can be performed with a single breath-hold and allows for reproducible T1 mapping for focal liver lesions, such as HCC, hemangioma, metastatic tumor, and cysts, before and after gadoxetic acid enhancement. T1 mapping using PSIR sequence is useful for differentiating focal liver lesions, which enables accurate diagnosis of focal liver lesions.

Ethical statement

All procedures performed in studies involving human participants were in accordance with the ethical standards of the institutional and/or national research committee (institutional review board of the Fukuoka University Chikushi Hospital) and with the 1964 Helsinki declaration and its later amendments or comparable ethical standards. Informed consent was obtained from all individual participants for the in vivo study.

Funding statement

This research did not receive any specific grant from funding agencies in the public, commercial, or not-for-profit sectors.

CRediT authorship contribution statement

Motohira Mio: Conceptualization, Data curation, Investigation, Methodology, Writing - original draft. **Yasuhiro Fujiwara:** Formal analysis, Software, Writing - review & editing. **Kazuki Tani:** Investigation. **Tatsuo Toyofuku:** Investigation. **Toshihiro Maeda:** Investigation. **Toshiro Inoue:** Investigation.

Declaration of Competing Interest

The authors report no declarations of interest.

References

[1] P. Reimer, E.J. Rummeny, H.E. Daldrup, et al., Enhancement characteristics of liver metastases, hepatocellular carcinomas, and hemangiomas with Gd-EOB-DTPA: preliminary results with dynamic MR imaging, Eur. Radiol. 7 (2) (1997) 275–280, https://doi.org/10.1007/s003300050150.

[2] M.K. Seale, O.A. Catalano, S. Saini, P.F. Hahn, D.V. Sahani, Hepatobiliary-specific MR contrast agents: role in imaging the liver and biliary tree, Radiographics 29 (6) (2009) 1725–1748, https://doi.org/10.1148/rg.296095515.

[3] C.S. van Kessel, W.B. Veldhuis, M.A.A.J. van den Bosch, M.S. van Leeuwen, MR liver imaging with gd-EOB-DTPA: a delay time of 10 minutes is sufficient for lesion characterisation, Eur. J. Radiol. 22 (10) (2012) 2153–2160, https://doi.org/10.1007/s00330-012-2486-2.

[4] Y. Takayama, A. Nishie, T. Nakayama, et al., Hypovascular hepatic nodule showing hypointensity in the hepatobikiary phase of gadoxetic acid-enhanced MRI in patients with chronic liver disease: prediction of malignant transformation, Eur. J. Radiol. 81 (11) (2012) 3072–3078, https://doi.org/10.1016/j.ejrad.2012.05.008.

[5] C.B. Sirlin, H.K. Hussain, E. Jonas, et al., Consensus report from the 6th international forum for liver MRI using gadoxetic acid, J. Magn. Reson. Imaging 40 (3) (2014) 516–529, https://doi.org/10.1002/jmri.24419.

[6] Y. Asayama, A. Nishie, K. Ishigami, et al., Distinguishing intrahepatic cholangiocarcinoma from poorly differentiated hepatocellular carcinoma using precontrast and gadoxetic acid-enhanced MRI, Diagn. Interv. Radiol. 21 (2) (2015) 96–104, https://doi.org/10.5152/dir.13013.

[7] N. Fujita, A. Nishie, Y. Asayama, et al., Significance of the signal intensity of gadoxetic acid-enhanced MR imaging for predicting the efficacy of hepatic arterial infusion chemotherapy in hepatocellular carcinoma, Magn. Reson. Med. Sci. 15 (1) (2016) 111–120, https://doi.org/10.2463/mrms.2015-0012.

[8] A.Y. Kim, Y.K. Kim, M.W. Lee, et al., Detection of hepatocellular carcinoma in gadoxetic acid-enhanced MRI and diffusion-weighted MRI with respect to the severity of liver cirrhosis, Acta radiol. 53 (8) (2012) 830–838, https://doi.org/10.1258/ar.2012.120099.

[9] T. Tamada, K. Ito, A. Yamamoto, et al., Hypointense hepatocellular nodules on hepatobiliary phase of Gd-EOB-DTPA-enhanced MRI: can increasing the flip angle improve conspicuity of lesions? J. Magn. Reson. Imaging 37 (5) (2013) 1093–1099, https://doi.org/10.1002/jmri.23903.

[10] K.I. Ringe, D.B. Husarik, C.B. Sirlin, E.M. Merkle, Gadoxetate disosium-enhanced MRI of the liver: part 1, protocol optimization and lesion appearance in the noncirrhotic liver, AJR Am. J. Roentgenol. 195 (1) (2010) 13–28, https://doi.org/10.2214/AJR.10.4392.

[11] S. Goshima, M. Kanematsu, H. Watanabe, et al., Hepatic hemangioma and metastasis: differentiation with gadoxetate disodium-enhanced 3-T MRI, AJR Am. J. Roentgenol. 195 (4) (2010) 941–946, https://doi.org/10.2214/AJR.09.3730.

[12] R. Golfieri, L. Grazioli, E. Orlando, et al., Which is the best MRI marker of malignancy for atypical cirrhotic nodules: hypointensity in hepatobiliary phase alone or combined with other features? Classification after Gd-EOB-DTPA administration, J. Magn. Reson. Imagimg 36 (3) (2012) 648–657, https://doi.org/10.1002/jmri.23685.

[13] T.J. Vogl, S. Kummel, R. Hammerstingl, et al., Liver tumors: comparison of MR imaging with Gd-EOB-DTPA and Gd-DTPA, Radiology 200 (1) (1996) 59–67, https://doi.org/10.1148/radiology.200.1.8657946.

[14] K. Saito, F. kotake, N. Ito, et al., Gd-EOB-DTPA enhanced MRI for hepatocellular carcinoma: quantitative evaluation of tumor enhancement in hepatobiliary phase, Magn. Reson. Med. Sci. 4 (1) (2005) 1–9, https://doi.org/10.2463/mrms.4.1.

[15] R.T. Gupta, D. Marin, D.T. Boll, et al., Hepatic hemangiomas: difference in enhancement pattern on 3T MR imaging with gadobenate dimeglumine versus gadoxetate disodium, Eur. J. Radiol. 81 (10) (2012) 2457–2462, https://doi.org/10.1016/j.ejrad.2011.10.014.

[16] H.S. Kim, D. Choi, S.H. Kim, et al., Changes in the signal- and contrast-to-noise ratios of hepatocellular carcinomas on gadoxetic acid-enhanced dynamic MR imaging, Eur. J. Radiol. 82 (1) (2013) 62–68, https://doi.org/10.1016/j.ejrad.2012.05.036.

[17] S.W. Farraher, H. Jara, K.J. Chang, A. Ozonoff, J.A. Soto, Differentiation of hepatocellular carcinoma and hepatic metastasis from cysts and hemangiomas with calculated T2 relaxation times and T1/T2 relaxation times ratio, J. Magn. Reson. Imaging 24 (6) (2006) 1333–1341, https://doi.org/10.1002/jmri.20758.

[18] N. Yoshimura, K. Saito, T. Saguchi, et al., Distinguishing hepatic hemangiomas from metastatic tumors using T1 mapping on gadoxetic-acid-enhanced MRI, Magn. Reson. Imaging 31 (1) (2013) 23–27, https://doi.org/10.1016/j.mri.2012.06.026.

[19] Z. Peng, C. Li, H. Cai, et al., Quantitative evaluation of Gd-EOB-DPA uptake in focal liver lesions by using T1 mapping: differences between hepatocellular carcinoma, hepatic focal nodular hyoerplasia and cavernous hemangioma, Oncotarget 8 (39) (2017) 65435–65444, https://doi.org/10.18632/oncotarget.18918.

[20] E.K. Fram, R.J. Herfkens, G.A. Johnson, et al., Rapid calculation of T1 using variable flip angke gradient refocused imaging, Magn. Reson. Imaging 5 (3) (1987) 201–208, https://doi.org/10.1016/0730-725x(87)90021-x.

[21] D.R. Messroghli, A. radjenovic, S. Kozerke, et al., Modified look-locker inversion recovery (MOLLI) for high-resolution T1 mapping of the heart, Magn. Reson. Med. 52 (1) (2004) 141–146, https://doi.org/10.1002/jmri.20110.

[22] Y. Fujiwara, H. Maruyama, N. Kosaka, Y. Ishimori, Simultaneous acquisition of high-contrast and quantitative liver T1 images using 3D phase-sensitive inversion recovery: a feasibility study, Acta radiol. 58 (8) (2017) 899–905, https://doi.org/10.1177/0284185116678273.

[23] P. Kellman, A.E. Arai, E.R. McVeigh, A.H. Aletras, Phase-sensitive inversion recovery for detecting myocardial infraction using gadolinium-delayed hyperenhancement, Magn. Reson. Med. 47 (2) (2002) 372–383, https://doi.org/10.1002/mrm.10051.

[24] A. Huber, K. Bauner, B.J. Wintersperger, et al., Phase-sensitive inversion recovery (PSIR) single-shot trueFISP for assessment of myocardial infraction at 3 tesla, Invest. Radiol. 41 (2) (2006) 148–153, https://doi.org/10.1097/01.rli.0000195843.97582.f4.

[25] P. Gowlang, P. Mansfield, P. Bullock, et al., Dynamic studies of gadolinium uptake in brain tumors using inversion-recovery echo-planar imaging, Magn. Reson. Med. 26 (2) (1992) 241–258, https://doi.org/10.1002/mrm.1910260206.

[26] K. Kamimura, Y. Fukukura, T. Yoneyama, et al., Quantitative evaluation of liver function with T1 relaxation time index on Gd-EOB-DTPA-enhanced MRI: comparison with signal intensity-based, J. Magn. Reson. Imaging 40 (4) (2014) 884–889, https://doi.org/10.1002/jmri.24443.

[27] Y. Ding, S.X. Rao, T. Meng, et al., Usefulness of T1 mapping on Gd-EOB-DTPA enhanced MR imaging in assessment of non-alcoholic fatty liver disease, Eur. Radiol. 24 (4) (2014) 959–966, https://doi.org/10.1007/s00330-014-3096-y.

[28] M. Onoda, T. Hyodo, T. Murakami, et al., Optimizing signal intensity correction during evaluation of hepatic parenchymal enhancement on gadoxetate disodium-enhanced MRI: comparison of three methods, Eur. J. Radiol. 84 (3) (2015) 339–345, https://doi.org/10.1016/j.ejrad.2014.11.014.

[29] A.S. Purysko, E.M. Remer, J.C. Veniero, Focal liver lesion detection and characterization with GD-EOB-DTPA, Clin. Radiol. 66 (7) (2011) 673–684, https://doi.org/10.1016/j.crad.2011.01.014.

[30] A. Kim, C.H. Lee, B.H. Kim, et al., Gadoxetic acid-enhanced 3.0T MRI for the evaluation of hepatic metastasis from colorectal cancer: metastasis is not always seen as a “defect” on the hepatobiliary phase, Eur. J. Radiol. 81 (12) (2012) 3998–4004, https://doi.org/10.1016/j.ejrad.2012.03.032.

[31] M.H. Yu, J.M. Lee, J.H. Yoon, et al., Clinical application of controlled aliasing in parallel imaging results in a higher acceleration (CAPIRINHA)-volumetric interpolated breathhold (VIBE) sequence for gadoxetic acid-enhanced liver MR imaging, J. Magn. Reson. Imaging 38 (5) (2013) 1020–1026, https://doi.org/10.1002/jmri.24088.

[32] J.K. Yoon, M.J. Kim, S. Lee, Compressed sensing and parallel imaging for double hepatic arterial phase acquisition in gadoxetate-enhanced dynamic liver magnetic resonance imaging, Invest. Radiol. 54 (6) (2019) 374–382, https://doi.org/10.1097/RLI.0000000000000548.